SEMARAK ILMU PUBLISHING

CFD Letters

Journal homepage:
https://semarakilmu.com.my/journals/index.php/CFD_Letters/index
ISSN: 2180-1363

Jet Impingement Cooling of a Microchannel Heat Sink with Microgroove

N.Y. Cheung[1], K.-C. Wong[1,*]

[1] Department of Mechanical, Materials and Manufacturing Engineering, University of Nottingham Malaysia, 43500, Malaysia

ARTICLE INFO

Article history:
Received 5 April 2023
Received in revised form 8 May 2023
Accepted 10 june 2023
Available online 1 December 2023

Keywords:
Jet impingement; microchannel heat sink; groove; cooling performance

ABSTRACT

The present study works on opportunities in improving the design of micro-channel heatsink (MCHS). The present study focuses on investigating numerically the effects of adding grooves at the MCHS which subject to jet impingement cooling. Commercial software ANSYS Fluent is used and realizable k-epsilon model is adopted to conduct a parametric study on the width and depth of rectangular longitudinal grooves at a constant heat flux of 250 W/cm2 applied at the base of MCHS. Two type of channel designs with grooves i.e. center-groove and side-groove were created and investigated numerically. Results show that addition of grooves generally give improvements in cooling performance and reducing the pressure drop. Some designs of side-grooved channels and center-grooved channels improve the temperature uniformity. The size of the groove affects the flow within the grooves and therefore affect the cooling performance.

1. Introduction

As electronics develop, their size decreases significantly overtime which leads to thermal issues such as overheating. Overheating is detrimental to the function of electronics as they often cause premature failure. Hence, this causes cooling systems to be heavily researched to match the pace of the advances of electronics.

An important breakthrough for small cooling systems happened with the proposal of the microchannel heat sink (MCHS) concept [1], capable of removing high heat flux while maintaining a small size.

This concept is simple in which multiple microchannels are machined onto a substrate. Coolant is then pumped through the channels which will absorb heat from the substrate. The concept pairs well with small electronics because it was found that its heat transfer coefficient (HTC) varies inversely with the width of each channel for laminar flow. This means that narrower channels could potentially perform better than wider ones, allowing this technology to be scaled down. When using water as a coolant, they were able to dissipate up to 790W/cm2 while having temperature rise of 71oC.

In 1997, it is shown that MCHS has 2 major disadvantages which is high pressure drop due to narrow channel width causing high pumping power to be required [2]. Furthermore, the increasing

* *Corresponding author.*
E-mail address: Kok-Cheong.Wong@nottingham.edu.my (K.-C. Wong)

https://doi.org/10.37934/cfdl.15.12.107116

fluid temperature and developing thermal boundary layer results in a high temperature difference between inlet and outlet. Therefore, they introduced the concept of manifold MCHS to decrease pressure drop. This was later studied in which the concept is found to decrease pressure drop by 35% [3]. However, the concept requires dividers which are bigger than the microchannel.

Over the years, a common approach to improve heat transfer is to introduce obstacles into the channel such as ribs which encourage hot and fluid mixing. However, ribs increase the pressure drop sharply due to their high intensity of flow disturbances [4]. Due to this, grooves have become widely used because they can disrupt and redevelop thermal boundary layers while minimising pressure drop [5].

Besides MCHS, grooves also provide benefits to jet impingement cooling which is a popular cooling method which dates back to before 1976 [6]. It cools a target by striking jets of high velocity fluid at the surface. In 2012, Liu et al., [7] studied the effects of using a grooved plate for multi-jet impingement. The results showed that adding grooves can enhance the heat transfer up to 15% when compared to a flat plate.

In 2003, Jang et al., [8] introduced a new concept where MCHS is subjected to an impinging air jet. The concept was found to have significantly reduced thermal resistance and pressure drop with improved temperature uniformity, minimizing the 2 main disadvantages of MCHS. Sung and Mudawar [9] later expanded upon the concept in 2006 and the single-phase heat transfer of a MCHS combined with slot jet impingement. However, MCHS with no fins (side walls) was used, causing a smaller contact area between solid and fluid regions and lower heat removal capability. Their numerical results obtained through k-Ɛ model agreed well with their experimental measurements. The accuracy of the model is supported by Baydar and Ozemen [10] where they proved the model is capable of predicting flow characteristics of confined jet impingement accurately.

In 2008, Sung and Mudawar [11] proceeded to investigate the heat transfer of the hybrid scheme with added fins. The sidewalls were found to improve heat removal significantly. While using coolant HFE-7100, the hybrid module is also found to maintain a highly uniform temperature and able to dissipate heat flux of 305.9W/cm2 under jet velocity of 7.37m/s. In their subsequent study of 2008 [12], the slot jet impingement was changed to a circular jet array. Having multiple jets allowed higher temperature uniformity than that of the slot jet. However, multiple jets also introduced crossflow which interferes with the heat transfer of downstream jets. The improvement brought by side walls was later confirmed by Kim et al., [13]. They compared the thermal performance between finned and finless hybrid schemes. Adding fins to the MCHS base were found to improve both heat transfer and temperature uniformity.

Using the finned hybrid scheme by Sung and Mudawar [12], Zhang et al., [14] numerically studied the effects of channel shapes on the cooling performance of the hybrid scheme in 2017. Their results showed that the cooling performance of a trapezoid channel is higher compared to those of rectangular and circular channels. Later in 2018, Zhang et al., [15] reused the trapezoid channel and numerically studied the effect of slot jet position on its cooling performance. They found out that the distance between the slot jet and the symmetry axis has a significant impact on maximum surface temperature and temperature uniformity.

Darwish *et al.,* [16] performed an experimental and numerical investigation on heat transfer enhancement and fluid flow characteristics of multiple free surface jet impingement using water and Al2O3-water nanofluid as coolants. They proposed correlation equations to calculate Nusselt number for both inline and staggered jets cooling system

During recent years, new hybrid scheme concepts are suggested by researchers. Barrau *et al.,* [17, 18] suggested a new hybrid scheme where the middle section of the channel is changed to an open plate. Results show that the concept improves temperature uniformity but sacrifices cooling

performance. In 2018, another concept is suggested by Robinson *et al.,* [19] in which the jet nozzles are extended into the channel. Numerical results showed that this hybrid module can dissipate heat flux up to 1000 W/cm^2 when using water as coolant. However, its complex geometry requires additive manufacturing for fabrication. It was then extended with experiments [20] and demonstrated one of the most effective thermal conductance levels at moderate pressure drop and flow rate.

Despite studies showing the benefits brought by grooves to MCHS and jet impingement, no studies have considered adding grooves to the hybrid scheme. Hence, the present study aims to numerically investigate the cooling effects of adding grooves with different geometric parameters to the base of channel for a MCHS subjected to jet impingement.

2. Methodology

Figure 1 shows the schematic of a hybrid cooling module of MCHS. Vertical slot jet impinges vertically at the top and exits the module from both ends horizontally. The substrate is made of copper with thermal conductivity, k_s of 387.6 Wm^{-1}. The coolant used is pure water. The module can be divided into many repeated sections of single channel as can be seen in Figure 1. The present study considers a quarter symmetry of a repeated section/ single channel as the computational domain as shown in Figure 2. The domain is divided into multiple rectangular blocks to allow ease of mesh refinement.

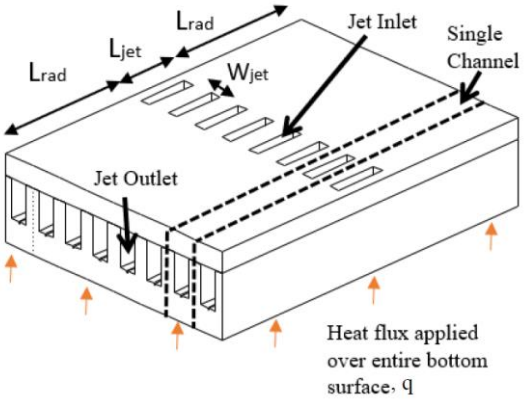

Fig. 1. Schematic of hybrid cooling module of slot jet impingement on MCHS

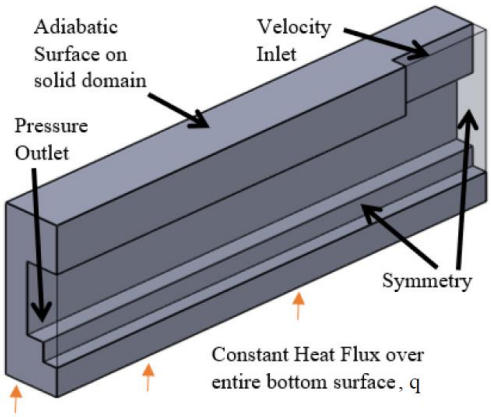

Fig. 2. Computational domain and boundary conditions on a quarter symmetry channel

ANSYS Fluent is used for the numerical simulation. 3D conjugate heat transfer analysis is carried out. The realizable k-epsilon model is applied in the present study as it is proven to be capable of accurately predicting turbulent flow and the vortices. The flow is assumed to be steady, single phase, turbulent and incompressible. Based on the above, the governing equations of continuity, momentum, energy are:

Continuity equation:

$$\nabla \cdot \vec{V} = 0 \tag{1}$$

Momentum equation:

$$\rho_f(\vec{V} \cdot \nabla)\vec{V} = -\nabla p + (\mu_f + \mu_t)\nabla^2\vec{V} \tag{2}$$

Energy equation for fluid:

$$\rho_f c_{p,f}(\vec{V} \cdot \nabla)T_f = (k_f + \frac{c_p \mu_t}{Pr_t})\nabla^2 T_f \tag{3}$$

Energy equation for solid:

$$k_s \nabla^2 T_s = 0 \tag{4}$$

The symbols ρ_f, μ_f, T_f , c_p, k_f and $\vec{V}$ denotes the fluid properties of density, viscosity, and specific heat, thermal conductivity, and velocity vector, respectively. The symbols k_s and T_s are the solid thermal conductivity and temperature, respectively. The turbulence parameters, Pr_t and μ_t are the turbulent Prandtl number and turbulent viscosity, respectively.

The boundary conditions applied are as follows:

i. Constant heat flux q of 250 W/cm^2 is applied to the bottom surface of the unit cell.
ii. At the solid-liquid interface, fluid and solid are thermally coupled so that temperature and heat flux are preserved over the interface.

$$T_s = T_f, k_s \frac{\partial T_s}{\partial n} = k_f \frac{\partial T_f}{\partial n} \tag{5}$$

iii. No slip is assumed at the solid-liquid interface.

$$u = v = w = 0 \tag{6}$$

iv. At the jet inlet.

$$u = w = 0, v = -u_{jet}, T = T_{in} \tag{7}$$

v. Pressure outlet boundary condition is used at the outlet with zero gauge pressure.
vi. Other surfaces are assumed to be adiabatic.

The effects of adding microgrooves are investigated by conducting a parametric analysis of grooves configurations as shown in Figure 3. Figure 3 shows the cross-sectional view of a vertical plane crossing inlet. In Figure 3, the left figure illustrates the plain flat channel, while the center figure illustrates the side-grooved channel which groove is added at the bottom corner of the channel, and the right one illustrates the center-grooved channel which groove is added at the center near the base of channel. The grooves added have a width of W_g, and a depth of D_g. Note that, for plain flat channel (left figure), $W_g = D_g = 0$.

The variables in this study are W_g and D_g, representing the width and depth of the groove, respectively. Note that each center-grooved channel has a groove width of $2W_g$ while each side-grooved channel has 2 grooves with a width of W_g each. Other parameters are constant with values of H_{jet}=1mm, H_{ch} =1.5mm, H_{bot}=1mm, W_{fin}=0.4$mmmm$ and W_{top}=0.3mm.

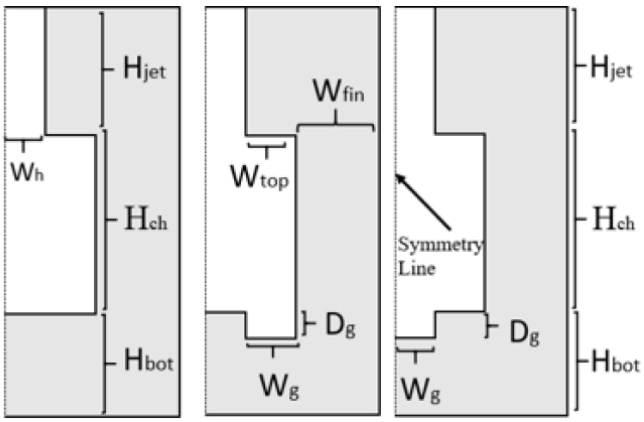

Fig. 3. Cross-section of domain for illustration of plain channel (left), side-grooved channel (center) and center-grooved channel (right)

The model is solved using SIMPLE algorithm [21] for pressure-velocity coupling. The convection-diffusion formulation of the momentum and energy equation of fluid are solved using second-order upwind scheme. A convergence criteria was set below 10^{-5} for the residuals. The parameters used to evaluate the performance of MCHS are described as follows:

Average base temperature:

$$\bar{T}_b = \frac{1}{A}\int T_b \, dA \tag{8}$$

where T_b is the local base temperature.

Pressure Drop:

$$\Delta P = \bar{T}_{inlet} - \bar{T}_{outlet} \tag{9}$$

where the pressure drop is mass-averaged.

Temperature uniformity is evaluated based on the maximum base temperature difference which is defined as:

$$\Delta T = T_{b,max} - T_{b,min} \tag{10}$$

where $T_{b,max}$ and $T_{b,min}$ are maximum and minimum temperatures at bottom surface of the hybrid module, respectively.

The jet Reynolds number is defined as:

$$Re = \frac{\rho u_{jet} D_{jet}}{\mu} \tag{11}$$

where the u_{jet} is the inlet jet velocity while hydraulic dynamic D_{jet} is:

$$D_{jet} = \frac{2L_{jet}W_{jet}}{L_{jet}+W_{jet}} \tag{12}$$

3. Results

The numerical model of the plain channel configuration is validated against the experimental results of Sung and Mudawar [11]. The results agree well with a maximum discrepancy of 5.31% for local base temperature as shown in Figure 4. A grid independence study is carried out on the grooved configurations. Mesh sizes of 1029600, 1360800 and 1646100 elements have been tested for the grooved configurations. Between the 2 finer meshes, the center-grooved and side-grooved channels have 0.26% and 0.37% change in average temperature while also having a 0.63% and 0.54% change in pressure drop respectively. Hence, the mesh size with 1360800 elements is chosen to generate results hereafter.

Numerical simulations have been conducted for various groove width. The results of $\bar{T}_b$ and ΔP for plain, center-grooved and side-grooved channels across different W_g are shown in Figure 5 for fixed values of D_g=0.2mm and Re=6341. The ranges of groove widths presented in Figure 5 are W_g = 0.0625—0.4375mm for center-grooved channels and W_g=0.1125—0.4785mm for side-grooved channels. In Figure 5, the result of plain flat channel (W_g = D_g = 0) is included as constant value for comparison. It can be observed in Figure 5(a) that, the side-grooved channels show relatively lower mean base temperature with the lowest mean temperature about 49°C at W_g = 0.3 mm, which is about 5.5 °C lower as compared to the plain channel. The effect of W_g on center-groove channel is relatively small, exhibiting value of between the plain flat channel and side-groove channels. This means both type of grooved channels give better cooling effect as compared to the plain channel, with side-grooved channel as the most superior. In Figure 5(b), the grooved channels also exhibit relatively lower ΔP as compared to the plain flat channel. In terms of pressure drop, center-grooved channels have the lowest pressure drop, but differences in ΔP are becoming smaller between both type of grooved channels for large values of W_g (W_g >0.35 mm).

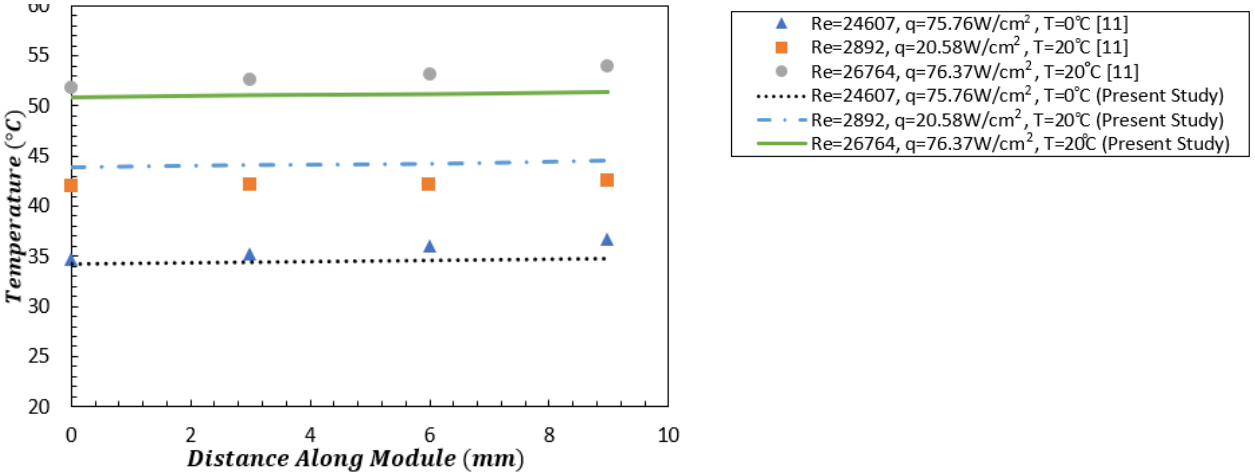

Fig. 4. Comparison of experimental results [11] and present numerical results obtained. T represents the temperature of the jet at the inlet.

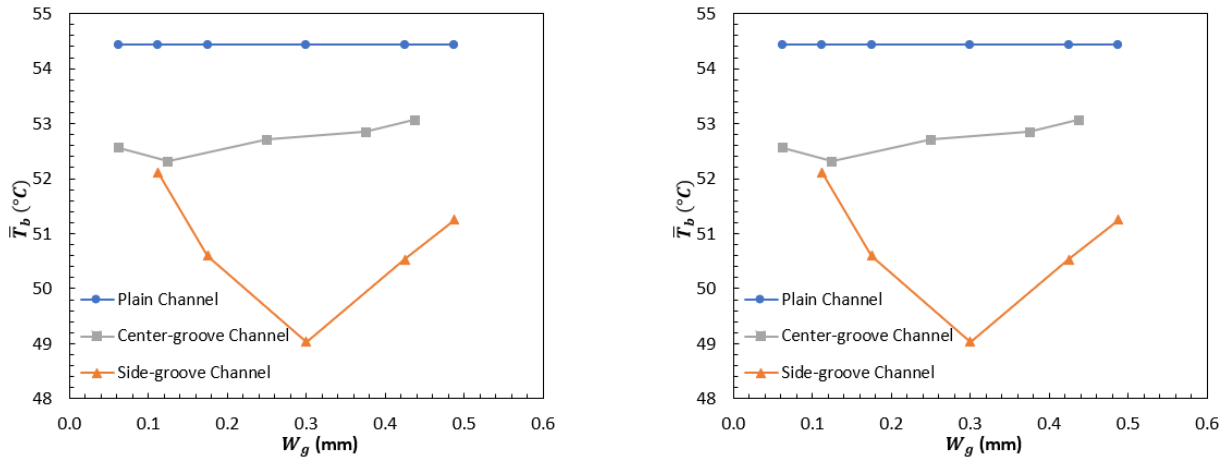

(a) (b)

Fig. 5. Variation of (a) $\bar{T}_b$ (left figure) and (b) ΔP with (D_g = 0.2mm fixed)

The effect of the depth of the grooves on $\bar{T}_b$ and ΔP have also been investigated. The results of $\bar{T}_b$ and ΔP for center-grooved and side-grooved channels for different D_g are shown in Figure 6 for fixed values of W_g= 0.3 mm and Re = 6341.

Figure 6(a) and Figure 6(b) clearly show that the increase in D_g reduces the value of $\bar{T}_b$ and ΔP for both type of grooves. This could be due to the larger flow passage when depth of groove become larger and enhances the heat transfer area. It can also be observed that the side-grooved channels give lower value of $\bar{T}_b$ as compared to the center-grooved channels but the other way round for the pressure drop as shown in Figure 6b. This mean the variation in mean temperature is in the reverse trend as the pressure drop. Further analysis on the flow is conducted to analyze this.

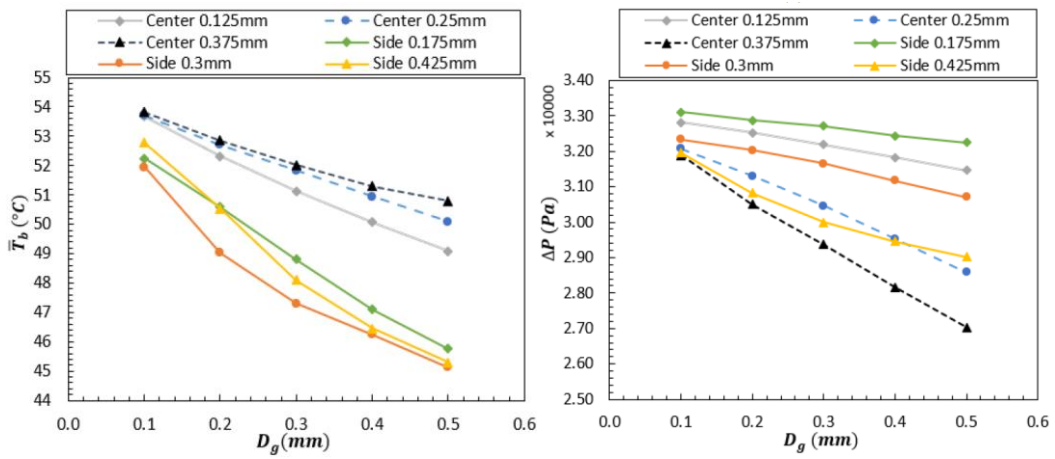

(a) (b)

Fig. 6. Variation of (a) $\bar{T}_b$ (left figure) and (b) ΔP with D_g (W_g = 0.3mm fixed)

The streamlines of various flow configurations are presented in Figure 7. The upper 5 figures in Figure 7(a) represents the flows for center-grooved channels for different W_g, whereas the lower 5 figures in Figure 7(b) represents the flows for side-grooved channels. From the streamlines, the figures show that, the flow slows down when reaches the grooves.

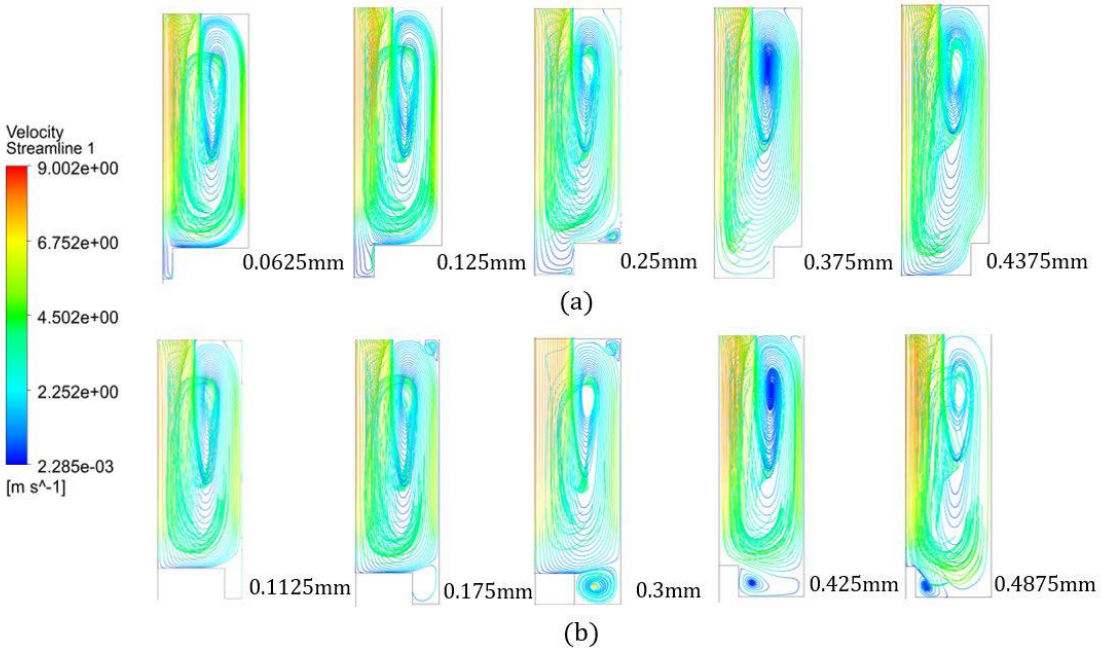

Fig. 7. Streamline plots of (a) Center-grooved Channels, (b) Side-grooved Channels

Generally, the grooves provide additional heat transfer area which contributes to better heat transfer regardless of the velocities of fluid within the grooves, however flow in the grooves affect how efficient heat can be transferred. For W_g = 0.3 mm in Figure 7(b), it can be seen that the fluid flow in the groove becomes strongest in which the circulation within the groove appears to be smooth and strong, and that explains why this figuration of side-grooved channel gives the best cooling. Note that the flow presented is at the mid vertical plane of the hybrid module. The flow at the mid plane affects the fluid mixing at the downstream along the channel. The flow patterns in Figure 7(a) generally show similar strength around the grooves among the center-grooved channels.

The temperature uniformity is also an important aspect of the cooling performance. In this study, the difference between the maximum and minimum temperature at the base of heatsink is evaluated as a measure of temperature uniformity. The smaller the difference, the better the temperature uniformity. The results are presented in Figure 8 for different value of W_g for both type of grooved-channels. The result for plain flat channel is also included for comparison. It can be seen in Figure 8 that, both the grooved channels exhibit value of ΔT_b lower than plain flat channel only at certain values of W_g. The results discussed implies that certain design of grooved channels are able to enhance the cooling effect in terms of mean temperature and temperature uniformity as well as reducing pressure drop relative to a plain flat channel.

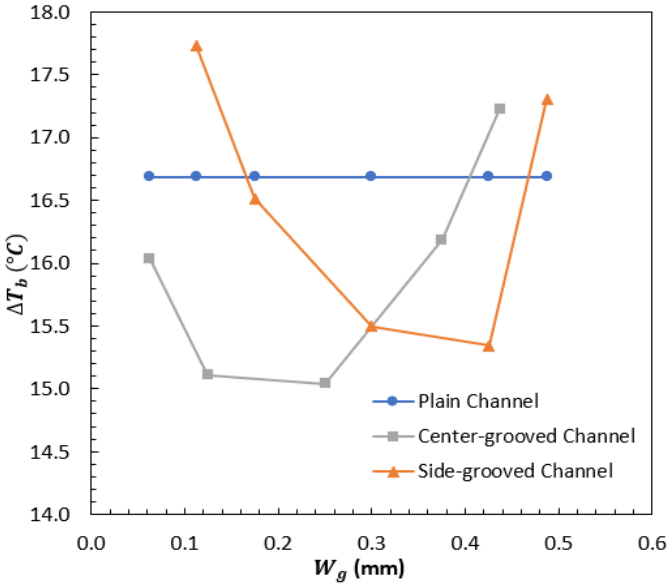

Fig. 8. Variation of ΔT_b with W_g at fixed $D_g = 0.2$ mm

4. Conclusions

The study on MCHS with different geometry of grooved channels subjected to jet impingement and a constant heat flux has been conducted numerically. The numerical model has been validated with a maximum discrepancy of 5.31% when compared to the experimental results in the literature. The present study numerically proved that adding grooves to the base of the channel generally improve cooling performance, and reduce pressure drop simultaneously when compared to a plain channel. MCHS with certain designs of grooved channels give better temperature uniformity as well. An optimal groove width of 0.3 mm of side-grooved channel was found to give lowest mean temperature at the heat sink base, and the streamlines of the fluid flow shows strong circulation within the groove.

Acknowledgement
This research was not funded by any grant.

References
[1] Tuckerman, David B., and Roger Fabian W. Pease. "High-performance heat sinking for VLSI." *IEEE Electron device letters* 2, no. 5 (1981): 126-129. https://doi.org/10.1109/EDL.1981.25367
[2] Copeland, D., Behnia, M. and Nakayama, W., 1997. Manifold microchannel heat sinks: isothermal analysis. IEEE Transactions on Components, Packaging, and Manufacturing Technology: Part A, 20(2), pp.96-102. https://doi.org/10.1109/95.588554

[3] Kim, Yong H., Woo Chong Chun, Jin Taek Kim, Bock Choon Pak, and Byoung Joon Baek. "Forced air cooling by using manifold microchannel heat sinks." *KSME International Journal* 12 (1998): 709-718. https://doi.org/10.1007/BF02945732
[4] Wang, Guilian, Nan Qian, and Guifu Ding. "Heat transfer enhancement in microchannel heat sink with bidirectional rib." *International Journal of Heat and Mass Transfer* 136 (2019): 597-609. https://doi.org/10.1016/j.ijheatmasstransfer.2019.02.018
[5] Bayrak, Ergin, Ali Bahadır Olcay, and Mustafa Fazıl Serincan. "Numerical investigation of the effects of geometric structure of microchannel heat sink on flow characteristics and heat transfer performance." *International journal of thermal sciences* 135 (2019): 589-600. https://doi.org/10.1016/j.ijthermalsci.2018.08.030
[6] Martin, Holger. "Heat and mass transfer between impinging gas jets and solid surfaces." In *Advances in heat transfer*, vol. 13, pp. 1-60. Elsevier, 1977. https://doi.org/10.1016/S0065-2717(08)70221-1
[7] Liu, Yao-Hsien, Siao-Jhe Song, and Yuan-Hsiang Lo. "Jet impingement heat transfer on target surfaces with longitudinal and transverse grooves." *International Journal of Heat and Mass Transfer* 58, no. 1-2 (2013): 292-299. https://doi.org/10.1016/j.ijheatmasstransfer.2012.11.042
[8] Jang, Seok Pil, Sung Jin Kim, and Kyung Wook Paik. "Experimental investigation of thermal characteristics for a microchannel heat sink subject to an impinging jet, using a micro-thermal sensor array." *Sensors and Actuators A: Physical* 105, no. 2 (2003): 211-224. https://doi.org/10.1016/S0924-4247(03)00103-1
[9] Sung, Myung Ki, and Issam Mudawar. "Experimental and numerical investigation of single-phase heat transfer using a hybrid jet-impingement/micro-channel cooling scheme." *International journal of heat and mass transfer* 49, no. 3-4 (2006): 682-694. https://doi.org/10.1016/j.ijheatmasstransfer.2005.08.021
[10] Baydar, E. R. T. A. N., and Y. Ü. C. E. L. Ozmen. "An experimental and numerical investigation on a confined impinging air jet at high Reynolds numbers." *Applied thermal engineering* 25, no. 2-3 (2005): 409-421. https://doi.org/10.1016/j.applthermaleng.2004.05.016
[11] Sung, Myung Ki, and Issam Mudawar. "Single-phase and two-phase cooling using hybrid micro-channel/slot-jet module." *International Journal of Heat and Mass Transfer* 51, no. 15-16 (2008): 3825-3839. https://doi.org/10.1016/j.ijheatmasstransfer.2007.12.015
[12] Sung, Myung Ki, and Issam Mudawar. "Single-phase hybrid micro-channel/micro-jet impingement cooling." *International Journal of Heat and Mass Transfer* 51, no. 17-18 (2008): 4342-4352. https://doi.org/10.1016/j.ijheatmasstransfer.2008.02.023
[13] Kim, Chol-Bom, Chuan Leng, Xiao-Dong Wang, Tian-Hu Wang, and Wei-Mon Yan. "Effects of slot-jet length on the cooling performance of hybrid microchannel/slot-jet module." *International Journal of Heat and Mass Transfer* 89 (2015): 838-845. https://doi.org/10.1016/j.ijheatmasstransfer.2015.05.108
[14] Zhang, Yanjun, Shuangfeng Wang, and Puxian Ding. "Effects of channel shape on the cooling performance of hybrid micro-channel and slot-jet module." *International journal of heat and mass transfer* 113 (2017): 295-309. https://doi.org/10.1016/j.ijheatmasstransfer.2017.05.092
[15] Zhang, Yanjun, Shuangfeng Wang, Kai Chen, and Puxian Ding. "Effect of slot-jet position on the cooling performance of the hybrid trapezoid channel and impingement module." *International Journal of Heat and Mass Transfer* 118 (2018): 1205-1217. https://doi.org/10.1016/j.ijheatmasstransfer.2017.11.054
[16] Darwish, Amr Mostafa, Abdel-Fattah Mohamed El-Kersh, Ibrahim Mahmoud El-Moghazy, and Mohamed Naguib Elsheikh. "Experimental and numerical study of multiple free jet impingement arrays with Al2O3-water nanofluid." *Journal of Advanced Research in Fluid Mechanics and Thermal Sciences* 65, no. 2 (2020): 230-252.
[17] Barrau, Jérôme, Daniel Chemisana, Joan Rosell, Lounes Tadrist, and Manuel Ibáñez. "An experimental study of a new hybrid jet impingement/micro-channel cooling scheme." *Applied Thermal Engineering* 30, no. 14-15 (2010): 2058-2066. https://doi.org/10.1016/j.applthermaleng.2010.05.013
[18] Barrau, Jérôme, Mohammed Omri, Daniel Chemisana, Joan Rosell, Manel Ibañez, and Lounes Tadrist. "Numerical study of a hybrid jet impingement/micro-channel cooling scheme." *Applied Thermal Engineering* 33 (2012): 237-245. https://doi.org/10.1016/j.applthermaleng.2011.10.001
[19] Robinson, A. J., R. Kempers, J. Colenbrander, N. Bushnell, and R. Chen. "A single phase hybrid micro heat sink using impinging micro-jet arrays and microchannels." *Applied Thermal Engineering* 136 (2018): 408-418. https://doi.org/10.1016/j.applthermaleng.2018.02.058
[20] Kempers, R., J. Colenbrander, W. Tan, R. Chen, and A. J. Robinson. "Experimental characterization of a hybrid impinging microjet-microchannel heat sink fabricated using high-volume metal additive manufacturing." *International Journal of Thermofluids* 5 (2020): 100029. https://doi.org/10.1016/j.ijft.2020.100029
[21] Suhas V.. Patankar. *Numerical heat transfer and fluid flow*. Hemisphere Publishing Corporation, 1980.